Electrical Energy Storage

Deutsche Ausgabe: DOI: 10.1002/ange.201505289
Internationale Ausgabe: DOI: 10.1002/anie.201505289

Cation-Dependent Stabilization of Electrogenerated Naphthalene Diimide Dianions in Porous Polymer Thin Films and Their Application to Electrical Energy Storage

Catherine R. DeBlase, Kenneth Hernández-Burgos, Julian M. Rotter, David J. Fortman, Dieric dos S. Abreu, Ronaldo A. Timm, Izaura C. N. Diógenes, Lauro T. Kubota, Héctor D. Abruña, and William R. Dichtel**

Abstract: *Porous polymer networks (PPNs) are attractive materials for capacitive energy storage because they offer high surface areas for increased double-layer capacitance, open structures for rapid ion transport, and redox-active moieties that enable faradaic (pseudocapacitive) energy storage. Here we demonstrate a new attractive feature of PPNs—the ability of their reduced forms (radical anions and dianions) to interact with small radii cations through synergistic interactions arising from densely packed redox-active groups, only when prepared as thin films. When naphthalene diimides (NDIs) are incorporated into PPN films, the carbonyl groups of adjacent, electrochemically generated, NDI radical anions and dianions bind strongly to K^+, Li^+, and Mg^{2+}, shifting the formal potentials of NDI's second reduction by 120 and 460 mV for K^+ and Li^+-based electrolytes, respectively. In the case of Mg^{2+}, NDI's two redox waves coalesce into a single two-electron process with shifts of 240 and 710 mV, for the first and second reductions, respectively, increasing the energy density by over 20 % without changing the polymer backbone. In contrast, the formal reduction potentials of NDI derivatives in solution are identical for each electrolyte, and this effect has not been reported for NDI previously. This study illustrates the profound influence of the solid-state structure of a polymer on its electrochemical response, which does not simply reflect the solution-phase redox behavior of its monomers.*

Developing efficient electrical energy storage devices (EESDs), whose design is grounded in fundamental electrochemical principles, is essential for utilizing and integrating intermittent sustainable energy sources into our energy portfolios.[1–4] Novel electrode materials and architectures for electrochemical supercapacitors and batteries are at the forefront of EESD research, which, despite similar design criteria, remain distinct applications because contemporary materials do not offer both high energy density, associated with batteries, and high power density, associated with capacitors. Organic materials represent attractive alternatives to metal oxide cathodes[1,2,5] because of their abundance, low cost, and tunable structures.[2,3,6–13] However, molecular compounds have lower volumetric energy densities and are often partially soluble in supporting electrolytes, compromising device performance and cyclability. Porous polymer networks (PPNs) are inherently insoluble, circumventing the dissolution limitation, and can store charge both faradaically, through charge-transfer processes of incorporated redox-couples,[14–18] and non-faradaically, by forming electrochemical double-layers.[19–23] Here we evaluate a PPN-functionalized electrode, which shows cation-dependent stabilization of redox-active dianions, providing increased cell voltages which, in turn, increase the energy density of EESDs.

An EESD's energy density scales with both its operating voltage, exhibiting a linear dependence for batteries and a squared dependence for capacitors, and its capacity. Both effects have been pursued with the intent of increasing EESD performance. Tuning the electrolyte's properties has gained increased interest since Gogotsi et al. reported increased capacitance when the pores of the electrode were similar in size to the electrolyte ions.[24] The ability to deliberately shift the reduction potentials of benzoquinone by changing the counter cation was first noted by Peover and Davies in 1963,[25] but this phenomenon has not since been exploited to deliberately tune a polymer electrode's redox potential.

Here we incorporate an NDI-containing monomer (**1**, Figure 1) into a PPN and demonstrate the dramatic difference in electrochemical response between the polymer film and **1** in solution. In this way, we examine how to deliberately and controllably shift the reduction potential of the NDI-containing PPN through ionic interactions with metal cations. The

[*] C. R. DeBlase,[+] K. Hernández-Burgos,[+] D. J. Fortman, Prof. H. D. Abruña, Prof. W. R. Dichtel
Chemistry and Chemical Biology, Cornell University
Ithaca, NY 14853-1301 (USA)
E-mail: hda1@cornell.edu
wdichtel@cornell.edu

J. M. Rotter
Department of Chemistry and Center for NanoScience (CeNS), University of Munich (LMU)
Butenandtstrasse 5–13, 81377 Munich (Germany)

D. S. Abreu, Prof. I. C. N. Diógenes
Departamento de Química Orgânica e Inorgânica
Universidade Federal do Ceará
Fortaleza, CE 60455-970 (Brazil)

R. A. Timm, L. T. Kubota
Department of Analytical Chemistry, Institute of Chemistry
Universidade Estadual de Campinas
13083 Campinas (Brazil)

[+] These authors contributed equally to this work.

Supporting information for this article is available on the WWW under http://dx.doi.org/10.1002/anie.201505289.

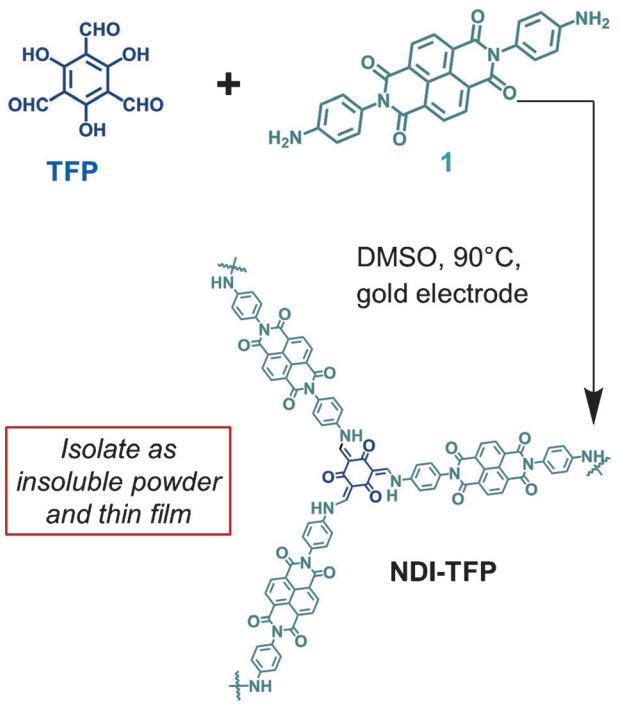

Figure 1. Solvothermal synthesis of the **NDI-TFP** polymer.

NDI polymer film exhibits counter cation-dependent electrochemical behavior, in which NDI's second reduction process is stabilized by as much as 710 mV, which we attribute to the close proximity of carbonyl groups of adjacent NDIs in the polymer film. In contrast, the solution electrochemistry of the NDI monomer does not change significantly as a function of the supporting electrolyte cation. This phenomenon, which has not been noted previously for porous polymers, or for NDI in any context, can enhance the operating voltages of EESDs, compared to those predicted from the electrochemical characterization of NDI in solution.

Triformylphloroglucinol (**TFP**) and **1** condense to form the **NDI-TFP** PPN as an insoluble, amorphous solid. The highest surface areas and optimal thin films were obtained through the slow addition of a **TFP** solution to a solution of **1** in DMSO (dimethylsulfoxide) (Figure 1). When three anilines react with **TFP**, the resulting imines tautomerize to provide β-ketoenamine functionalities, a behavior that has been observed in small organic compounds,[26] other PPNs,[27] and covalent organic frameworks (COFs).[28] In extended networks, this linkage provides materials that are oxidatively and hydrolytically robust.[10,28–30] The FTIR spectrum of the polymer indicates that it is linked by β-ketoenamines, as evidenced by the disappearance of the N–H stretches, the appearance of a characteristic C–N stretch at 1250 cm^{-1} and a C=C stretch at 1560 cm^{-1}, and the shifting of the C=O stretch from 1660 cm^{-1} to 1615 cm^{-1} (Figure S4 in the Supporting Information). ^{13}C cross-polarization magic angle spinning (CP-MAS) solid-state NMR spectroscopy also indicates the formation of β-ketoenamine-linked materials, as the spectrum of **NDI-TFP** exhibits resonances at 145 ppm that correspond to the enamine carbon (=CNH) and α-carbon at 115 ppm (Figure S3). Furthermore, the **TFP** aldehyde resonance at 193 ppm is replaced by a peak at 180 ppm, corresponding to the ketone resonance. High-resolution X-ray photoelectron spectroscopy (XPS) shows a clear shift of the N 1s signal for monomer **1** at 401.01 eV, corresponding to its aniline-type moieties, to 398.45 eV for the enamines of the **NDI-TFP** polymer, which is consistent with shifts observed for other β-ketoenamine-linked materials (Figure S6). **NDI-TFP** polymers prepared under conditions in which the monomers are fully soluble, a condition that provided superior surface areas for related materials,[10,31] exhibited Brunauer–Emmett–Teller (BET) surface areas of $414 \pm 188\ m^2 g^{-1}$ with a total pore volume of $0.19 \pm 0.02\ cm^3 g^{-1}$ (average of four samples) with a highest value of $790\ m^2 g^{-1}$ (Figure S7).

We also prepared the **NDI-TFP** polymer as a thin film on gold electrodes because in a previous study we observed that 2D COF thin films exhibited superior electrochemical performance compared to insoluble powders.[30] Film deposition on electrode surfaces was achieved by including an electrode (Au) in a DMSO solution of **1** and slowly introducing a **TFP**-containing solution over the course of 1 h. After 12 h, yellow films with a fibrous morphology (Figure S5) were obtained. **NDI-TFP** polymer films exhibited similar FTIR and XPS spectra to those discussed above (Figure S4 and S6). These films were characterized electrochemically, and compared to the performance of monomer **1** in solution. The porous, high surface area nature of the **NDI-TFP** thin films was confirmed qualitatively by observing enhanced Kr adsorption by polymer films relative to unmodified Au substrates. (Figure S9).

NDI undergoes two one-electron reduction processes to yield a radical anion and dianion (Figure 2), respectively, each of which might interact with cations of differing charge and size.[32] **NDI-TFP** polymer thin films on gold electrodes

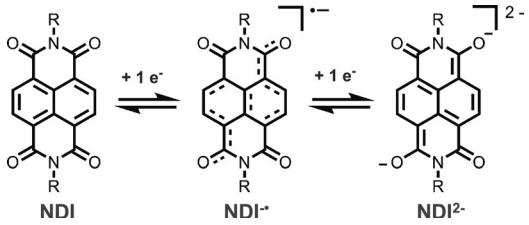

Figure 2. Reduction and oxidation processes for naphthalene diimide moieties.

exhibit distinct and counter cation-dependent electrochemical behavior (Figure 3B) that is not observed for solutions of **1** (Figure 3A). No cation dependence was observed in the reduction of the NDI monomer **1** in DMSO solution using cyclic voltammetry (CV, Figure 3A). The two one-electron redox processes for all electrolyte cations occurred at $E^{\circ\prime} = -0.95$ V and -1.41 V vs $Ag/AgClO_4$, respectively. The **NDI-TFP** polymer exhibits a similar electrochemical response to that of monomer **1** in the presence of bulky, non-interacting tetrabutylammonium (TBA^+) cations (Figure 3B).[9] Two one-electron processes with formal potentials of -0.96 and -1.43 V vs $Ag/AgClO_4$ are observed. Since there were

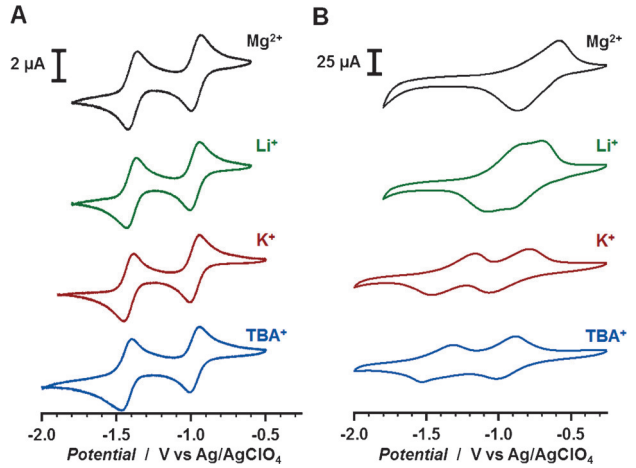

Figure 3. A) Cyclic voltammograms of **1** (10 mV s^{-1}, DMSO, 0.1 M perchlorate supporting electrolyte), TBA$^+$ = tetrabutylammonium. B) Cyclic voltammograms of **NDI-TFP** polymer films on Au electrodes (10 mV s^{-1}, CH_3CN, 0.1 M perchlorate supporting electrolyte).

minimal interactions between the **NDI** and the TBA$^+$, the formal potentials remained essentially invariant and were the most negative (Figure 3B, Table 1). This response indicates that TBA$^+$ does not interact with the NDI radical anion or dianion strongly. However, the **NDI-TFP** polymer's formal potentials shift to more positive values in the presence of the smaller cations Li$^+$ and K$^+$ (K$^+$ at $E^{\circ\prime}_1 = -0.93$ V, $E^{\circ\prime}_2 = -1.31$ V and Li$^+$ at $E^{\circ\prime}_1 = -0.83$ V, $E^{\circ\prime}_2 = -0.97$ V vs Ag/$AgClO_4$) (Figure 3B and Table 1). These smaller, higher charge density cations interact strongly with NDI^{2-} and stabilize it, as indicated by the shift in its response to more positive potentials relative to TBA$^+$. This trend was also confirmed using in situ confocal Raman spectroscopy (see Supporting Information).

Table 1: The formal potentials for the **NDI-TFP** polymer are shifted to positive potentials as a consequence of ionic interactions.[a]

Cation **1**	$E^{\circ\prime}_{R1}$	$E^{\circ\prime}_{R2}$	$\Delta E^{\circ\prime}_{R1}$	$\Delta E^{\circ\prime}_{R2}$
TBA$^+$	−0.96	−1.43	n/a	n/a
K$^+$	−0.93	−1.31	0.03	0.12
Li$^+$	−0.83	−0.97	0.13	0.46
Mg^{2+}	−0.72	−0.72	0.24	0.71

[a] $E^{\circ\prime}_{RX}$ = reduction, where $x = 1$ is first reduction and $x = 2$ is second reduction. All potentials are reported as V vs Ag/$AgClO_4$.

Even greater stabilization of NDI^{2-} within the polymer film is observed for Mg^{2+}, such that both waves merge into a single two-electron process at a formal potential of −0.72 V vs Ag/$AgClO_4$. The redox potential was also shifted positively by Al^{3+}, but the electrochemistry was irreversible (Figure S16). This experiment suggests that a triply charged cation binds strongly to the dense network of dianions and that there are presumably significant steric effects that influence the screening of the trication. The shift in the formal potentials for Mg^{2+} corresponds to an increase in energy density of more than 20% for the polymer. We have noted effects of this magnitude in other carbonyl-containing redox systems in solution,[8,9] but this is the first observation of this behavior in polymer films or for NDI in any context, despite its extensive use as a redox-active moiety in molecular and polymeric systems. Furthermore, all electrolytes yielded chemically reversible responses, as evidenced by the equal peak currents for each redox process, which is essential for devices to maintain their performance after extensive cycling. We attribute this feature to the polymer's high stability and insolubility, which suppress degradation of the electroactive moieties. The chemical reversibility of the NDI^{2-}/Mg^{2+} species is also notable, because the corresponding reduction in most carbonyl-based redox couples is irreversible.[33] Inspired by the calculated increase in energy density for **NDI-TFP**/Mg^{2+}, we examined the charge/discharge profiles for **NDI-TFP** thin films in the presence of each of the cations (as perchlorate salts) studied to determine their charge storage capacities (Figure 4, S13, and S14). At a current of 70 μA, all films exhibited well behaved charge/discharge profiles with capacities around 100 mA h g^{-1} (see Supporting Information for details). The profiles exhibited well-defined plateaus at potentials corresponding to the redox processes (as determined from cyclic voltammetry). In addition, the profiles confirm the increase in energy density.

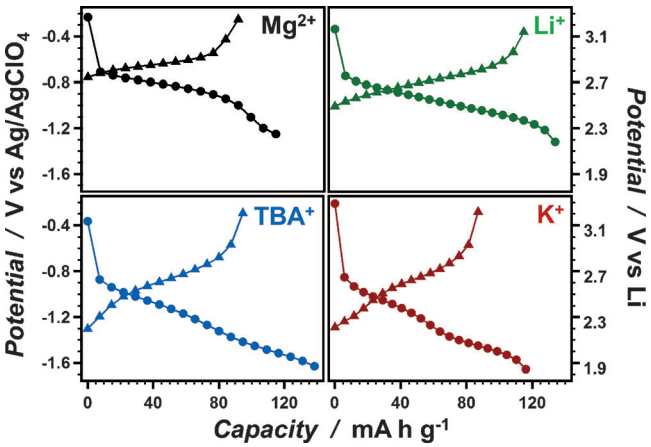

Figure 4. Potential–capacity profiles, at a current of 70 μA, of **NDI-TFP** films in various perchlorate electrolytes, where ● represents charge (generation of NDI^{2-}) and ▲ represents discharge (generation of NDI). The right axis shows potentials relative to Li.

These electrochemical studies highlight the importance of polymer morphology for optimizing ionic interactions and, in turn, the application of these materials for EESDs. The porous nature of **NDI-TFP** allows the cations to be held within the pores to stabilize the dianion. For NDI in solution, the standard rate constant ($k^{\circ\prime}$) for electron transfer was determined, using the Nicholson method,[34] to be 3×10^{-3} cm s^{-1} for all electrolytes, which is characteristic of quasireversible processes. The same analysis was performed on the **NDI-TFP** polymer deposited onto a microelectrode ($r = 30$ μm) to mitigate ohmic drops. The obtained $k^{\circ\prime}$ values were 4×10^{-3} cm s^{-1}, 3×10^{-3} cm s^{-1}, 6×10^{-4} cm s^{-1} and 6×10^{-4} cm s^{-1} for TBA$^+$, K$^+$, Li$^+$, and Mg^{2+} respectively. The

variations ($TBA^+ > K^+ > Li^+ \approx Mg^{2+}$) in the standard rate constant values may reflect electrostatic effects. These observations demonstrate that, in materials design, the properties of the monomers cannot necessarily be used to predict the behavior of the polymeric form.

The diffusion coefficients of the cations through **NDI-TFP** films were determined using chronoamperometry by stepping the potential to −1.8 V vs $Ag/AgClO_4$ and monitoring the current response (Figure S12 and Table S1). The current plotted against the inverse square root of time (Cotrell plot) in each electrolyte is indicative of finite diffusion processes (i.e., those of surface bound redox couples). The smallest (Li^+) and largest (TBA^+) cations diffuse most quickly through the polymer films at 1.2×10^{-11} and 2.3×10^{-11} $cm^2 s^{-1}$, respectively. We attribute these responses to a non-interacting cation, which is too large to bind well to the reduced **NDI**, in the case of TBA^+, or, for Li^+, an ion that is too small to be restricted within the **NDI-TFP** polymer matrix. The diffusion coefficient of Mg^{2+} is three times smaller than that of Li^+ (0.4×10^{-11} $cm^2 s^{-1}$), which we attribute to enhanced coulombic interactions between the reduced NDI and the Mg^{2+} ion. Although somewhat speculative, we propose that the local structure of the **NDI-TFP** polymer places carbonyls of adjacent NDI units sufficiently close for the Mg^{2+} dication to stabilize both anions at once. These interactions would be stronger than those of Li^+ and further restrict diffusion. K^+ showed the smallest diffusion coefficient at 0.3×10^{-11} $cm^2 s^{-1}$, although this response may be influenced by resistance effects arising from the limited solubility of this electrolyte. In all cases, we attribute the slow diffusion to a combination of ionic interactions and blocked pores or torturous pathways that hinder ions moving throughout the material.

We employed electrochemical impedance spectroscopy (EIS) in CH_3CN using the ClO_4^- salts of TBA^+, Li^+, K^+, and Mg^{2+} to further characterize the electrical conductivity and charge transport behavior of the films. EIS was performed at −0.2, −1.0 and −1.4 V, at which the NDI is present as the neutral, anion radical, and dianion, respectively. Using a two constant phase element (2CPE) model in series with the solution resistance (R_{sol}, where $R_{sol} \approx 800\ \Omega$), we extracted the charge transfer resistances associated with the reduction of the NDI units, which was lowest at −1.0 V applied potential for each ion. Our interpretation of this phenomenon is that the film is in effect "mixed valent". Thus, redox conduction can enhance the effective rate of charge transfer, providing lower values of R_{CT}. A more extensive discussion of the impedance data is presented in the supplementary information section. Strategies to enhance charge transfer in porous polymers, even when electrical conductivity is limited, broadens the scope of potential polymers usable in energy storage, while maximizing their performance.

In conclusion, we synthesized a robust, NDI-containing, β-ketoenamine-linked polymer network, both as a high surface area powder and as a thin film. Its reduction processes are stabilized by coordinating cations of the supporting electrolyte, an effect that is not observed for the NDI monomer in solution or previously reported for NDI-containing polymers or assemblies. We attribute this behavior to the ability of NDI dianions to strongly bind K^+, Li^+, and Mg^{2+} in the polymer films, shifting its formal reduction potentials. The largest effect is observed for Mg^{2+}, which induces the coalescence of NDI's two redox waves into a single two-electron reduction at more positive potentials (a shift of 710 mV). Although the diffusion coefficients for all of the ions were small (10^{-11} $cm^2 s^{-1}$), non-interacting TBA^+ cations diffused most rapidly through the **NDI-TFP** polymer. These studies demonstrate that, although solution-phase characterization is effective for assessing the number of electrons transferred and/or approximate location of redox potentials, it does not necessarily indicate how electron transfer will occur in polymer thin films. These results illustrate the importance of microstructure in electrochemical behavior in general, and electrical energy storage in particular. Harnessing these potential shifts is also of technological interest, as they give rise to higher operating voltages for EESDs than would be expected from solution studies, which can significantly increase their energy densities.

Acknowledgements

This research was supported by an NSF GRFP (DGE-1144153) award to C.R.D. W.R.D. acknowledges support from the Alfred P. Sloan and Camille and Henry Dreyfus Foundations. This work was supported in part (K.H.B., H.D.A.) through grant DE-FG02-87ER45298, by the Energy Materials Center at Cornell (emc^2), an Energy Frontier Research Center funded by the DOE Office of Basic Energy Sciences (DE-SC000001086) and an Innovation Economy Matching Grant from the New York State, Empire State Development Division of Science, Technology and Innovation (NYSTAR), under contract number C090148. R.A.T. acknowledges Sao Paulo Research Foundation for BEPE-PD Fellowship (2013/25527-1). This research made use of the Cornell Center for Materials Research Facilities supported by the NSF (DMR-1120296) and Nanobiotechnology Center.

Keywords: electrical energy storage devices · electrochemistry · porous polymers · redox processes · supercapacitors

How to cite: *Angew. Chem. Int. Ed.* **2015**, *54*, 13225–13229
Angew. Chem. **2015**, *127*, 13423–13427

[1] J. B. Goodenough, H. D. Abruña, M. V. Buchanan, *Basic Research Needs for Electrical Energy Storage*, Office Of Basic Sciences, US Department Of Energy, **2007**.
[2] Z. Song, H. Zhou, *Energy Environ. Sci.* **2013**, *6*, 2280–2301.
[3] S. E. Burkhardt, M. A. Lowe, S. Conte, W. Zhou, H. Qian, G. G. Rodríguez-Calero, J. Gao, R. G. Hennig, H. D. Abruña, *Energy Environ. Sci.* **2012**, *5*, 7176–7187.
[4] P. Poizot, F. Dolhem, *Energy Environ. Sci.* **2011**, *4*, 2003–2019.
[5] P. Simon, Y. Gogotsi, *Nat. Mater.* **2008**, *7*, 845–854.
[6] H. Chen, M. Armand, G. Demailly, F. Dolhem, P. Poizot, J.-M. Tarascon, *ChemSusChem* **2008**, *1*, 348–355.
[7] Y. NuLi, Z. Guo, H. Liu, J. Yang, *Electrochem. Commun.* **2007**, *9*, 1913–1917.
[8] K. Hernández-Burgos, S. E. Burkhardt, G. G. Rodríguez-Calero, R. G. Hennig, H. D. Abruña, *J. Phys. Chem. C* **2014**, *118*, 6046–6051.

[9] K. Hernández-Burgos, G. G. Rodríguez-Calero, W. Zhou, S. E. Burkhardt, H. D. Abruña, *J. Am. Chem. Soc.* **2013**, *135*, 14532 – 14535.
[10] C. R. DeBlase, K. E. Silberstein, T.-T. Truong, H. D. Abruña, W. R. Dichtel, *J. Am. Chem. Soc.* **2013**, *135*, 16821 – 16824.
[11] F. Xu, H. Xu, X. Chen, D. Wu, Y. Wu, H. Liu, C. Gu, R. Fu, D. Jiang, *Angew. Chem. Int. Ed.* **2015**, *54*, 6814 – 6818; *Angew. Chem.* **2015**, *127*, 6918 – 6922.
[12] F. Xu, S. Jin, H. Zhong, D. Wu, X. Yang, X. Chen, H. Wei, R. Fu, D. Jiang, *Sci. Rep.* **2015**, *5*, 1 – 6.
[13] F. Xu, X. Chen, Z. Tang, D. Wu, R. Fu, D. Jiang, *Chem. Commun.* **2014**, *50*, 4788 – 4790.
[14] Y. Wang, Y. Bai, X. Li, Y. Feng, H. Zhang, *Chem. Eur. J.* **2013**, *19*, 3340 – 3347.
[15] J. Benson, S. Boukhalfa, A. Magasinski, A. Kvit, G. Yushin, *ACS Nano* **2012**, *6*, 118 – 125.
[16] L.-Q. Mai, A. Minhas-Khan, X. Tian, K. M. Hercule, Y.-L. Zhao, X. Lin, X. Xu, *Nat. Commun.* **2013**, *4*, 1 – 7.
[17] N. Kurra, N. A. Alhebshi, H. N. Alshareef, *Adv. Energy Mater.* **2014**, 1401303 – 1401303.
[18] H. Huang, L. F. Nazar, *Angew. Chem. Int. Ed.* **2001**, *40*, 3880 – 3884; *Angew. Chem.* **2001**, *113*, 3998 – 4002.
[19] E. Frackowiak, F. Béguin, *Carbon* **2001**, *39*, 937 – 950.
[20] Y. Gu, Z. Xiong, W. A. Abdulla, G. Chen, X. S. Zhao, *Chem. Commun.* **2014**, *50*, 14824 – 14827.
[21] N.-S. Choi, Z. Chen, S. A. Freunberger, X. Ji, Y.-K. Sun, K. Amine, G. Yushin, L. F. Nazar, J. Cho, P. G. Bruce, *Angew. Chem. Int. Ed.* **2012**, *51*, 9994 – 10024; *Angew. Chem.* **2012**, *124*, 10134 – 10166.
[22] H. D. Abruña, Y. Kiya, J. C. Henderson, *Phys. Today* **2008**, *61*, 43 – 47.
[23] Y. Zhai, Y. Dou, D. Zhao, P. F. Fulvio, R. T. Mayes, S. Dai, *Adv. Mater.* **2011**, *23*, 4828 – 4850.
[24] J. Chmiola, G. Yushin, Y. Gogotsi, C. Portet, P. Simon, P. L. Taberna, *Science* **2006**, *313*, 1760 – 1763.
[25] M. E. Peover, J. D. Davies, *J. Electroanal. Chem.* **1963**, *6*, 46 – 53.
[26] J. H. Chong, M. Sauer, B. O. Patrick, M. J. MacLachlan, *Org. Lett.* **2003**, *5*, 3823 – 3826.
[27] Y. Zhu, W. Zhang, *Chem. Sci.* **2014**, *5*, 4957 – 4961.
[28] S. Kandambeth, A. Mallick, B. Lukose, M. V. Mane, T. Heine, R. Banerjee, *J. Am. Chem. Soc.* **2012**, *134*, 19524 – 19527.
[29] S. Kandambeth, D. B. Shinde, M. K. Panda, B. Lukose, T. Heine, R. Banerjee, *Angew. Chem. Int. Ed.* **2013**, *52*, 13052 – 13056; *Angew. Chem.* **2013**, *125*, 13290 – 13294.
[30] C. R. DeBlase, K. Hernández-Burgos, K. E. Silberstein, G. G. Rodríguez-Calero, R. P. Bisbey, H. D. Abruña, W. R. Dichtel, *ACS Nano* **2015**, *9*, 3178 – 3183.
[31] B. J. Smith, W. R. Dichtel, *J. Am. Chem. Soc.* **2014**, *136*, 8783 – 8789.
[32] N. Gupta, H. Linschitz, *J. Am. Chem. Soc.* **1997**, *119*, 6384 – 6391.
[33] E. Levi, Y. Gofer, D. Aurbach, *Chem. Mater.* **2010**, *22*, 860 – 868.
[34] R. S. Nicholson, *Anal. Chem.* **1965**, *37*, 1351 – 1355.

Received: June 9, 2015
Revised: July 29, 2015
Published online: September 10, 2015

